Polymer Chemistry

PAPER

View Article Online
View Journal | View Issue

Cite this: *Polym. Chem.*, 2015, **6**, 6001

Biocompatible and bioreducible micelles fabricated from novel α-amino acid-based poly(disulfide urethane)s: design, synthesis and triggered doxorubicin release†

Wentao Lu, Xiuxiu Wang, Ru Cheng,* Chao Deng, Fenghua Meng and Zhiyuan Zhong*

Received 31st May 2015,
Accepted 28th June 2015

DOI: 10.1039/c5py00828j

www.rsc.org/polymers

α-Amino acid-based functional biopolymers are highly appealing for various biomedical applications including controlled drug delivery. In this paper, we report the design and development of novel reductively biodegradable α-amino acid-based poly(disulfide urethane)s, denoted as AAPU(SS)s, as well as PEG-AAPU(SS)-PEG triblock copolymer micelles for triggered intracellular doxorubicin (DOX) release. AAPU(SS)s were synthesized with controlled M_n ranging from 4.6 to 35.7 kg mol^{-1} *via* polycondensation reaction between two α-amino acid derivatives, disulfide-linked bis(ethyl L-serinate) (SS-BSER) and L-lysine ethyl ester diisocyanate (LDI). AAPU(SS)s are amorphous with a glass transition temperature (T_g) of 31.7–49.2 °C and were degraded into low molecular weight fragments under a reductive condition. PEG-AAPU(SS)-PEG copolymer could be readily obtained by treating AAPU(SS) with mPEG-NCO. PEG-AAPU(SS)-PEG formed micelles with a mean diameter of 155 nm. The *in vitro* release studies showed that drug release from DOX-loaded PEG-AAPU(SS)-PEG micelles was significantly accelerated in the presence of 10 mM glutathione (GSH). MTT assays revealed that DOX-loaded PEG-AAPU(SS)-PEG micelles caused effective growth inhibition of both RAW 264.7 and drug resistant MCF-7 cells (MCF-7/ADR) while the corresponding blank micelles were non-cytotoxic even at a high concentration of 1.0 mg mL^{-1}. Confocal microscopy showed that PEG-AAPU(SS)-PEG micelles efficiently transported and released DOX into the perinuclear and nuclear regions of MCF-7/ADR cells. These biocompatible and bioreducible α-amino acid-based poly(disulfide urethane) micelles have appeared to be a particularly interesting platform for triggered intracellular anticancer drug delivery.

Introduction

α-Amino acid-based functional biopolymers such as polypeptides, polydepsipeptides and α-amino acid-based poly(ester amide)s are highly appealing for various biomedical applications including tissue engineering and controlled drug delivery.[1–5] Unlike most other polymers, α-amino acid-based biopolymers typically possess excellent cell and tissue compatibility. Moreover, they would eventually be degraded into α-amino acids and derivatives, which do not pose any toxicity concerns. The synthesis of α-amino acid-based functional biopolymers, however, often requires involved synthesis and stringent purification processes. In comparison, polyurethanes (PUs) are a robust and versatile family of polymers that are conveniently prepared from polycondensation of diols with diisocyanates under mild conditions.[6–8] PUs exhibit excellent physical properties and biocompatibility and have been widely used in biomedical implants.[9–11] In recent years, biodegradable PUs have been prepared based on aliphatic polyesters and polycarbonates for drug delivery applications.[12–16]

It is found that drug release from common biodegradable polymeric nanoparticles is generally slow and incomplete, leading to compromised therapeutic efficacy *in vitro* and *in vivo*.[17] In order to achieve enhanced drug release, various stimuli-sensitive polymeric nanoparticles have been developed.[18–20] In particular, reduction-sensitive polymeric nanoparticles have attracted growing interest for cytoplasmic anticancer drug delivery in that there is a high reducing potential in the

Biomedical Polymers Laboratory, and Jiangsu Key Laboratory of Advanced Functional Polymer Design and Application, College of Chemistry, Chemical Engineering and Materials Science, Soochow University, Suzhou, 215123, P. R. China.
E-mail: rcheng@suda.edu.cn, zyzhong@suda.edu.cn

†Electronic supplementary information (ESI) available. See DOI: 10.1039/c5py00828j

cytosols of cancer cells.[21] The work from different research groups has revealed that reduction-sensitive shell-sheddable micelles,[22–27] main chain degradable nanoparticles[28–32] and reversibly crosslinked polymeric nanocarriers[33–36] display significantly improved *in vitro* and *in vivo* anticancer efficacy as compared to the non-sensitive counterparts. Tan *et al.* reported that reduction-sensitive multiblock PU micelles based on bis(2-hydroxyethyl) disulfide, L-lysine ethyl ester diisocyanate (LDI) and poly(ε-caprolactone) (PCL) released 60% of PTX under a reductive condition containing 10 mM glutathione (GSH) in 48 h while only about 10% of PTX was released under a non-reductive condition, exhibiting enhanced *in vitro* anticancer effects against HepG2 cells.[37] pH and reduction dual sensitive PEG/PU nanoparticles in which PU was prepared by polycondensation of bis-1,4-(hydroxyethyl)piperazine, bis(2-hydroxyethyl) disulfide and 1,6-hexamethylene diisocyanate (HDI) displayed efficient growth inhibition of HeLa and HepG2 cells *in vitro*.[38] It should be noted that bis(2-hydroxyethyl) disulfide might pose potential cytotoxicity concerns. Chen *et al.* recently reported that disulfide crosslinked PU micelles exhibited a better antitumor efficacy with reduced toxicity in the nude mice bearing HepG2 tumor xenografts as compared with free DOX and the non-crosslinked counterpart.[39] Notably, there is no report on the development of α-amino acid-based biocompatible and reductively degradable PUs and their amphiphilic block copolymer micelles for controlled drug delivery.

In this paper, novel α-amino acid-based biocompatible and bioreducible poly(disulfide urethane)s, denoted as AAPU(SS)s, and PEG-AAPU(SS)-PEG triblock copolymer micelles were designed, prepared and investigated for triggered intracellular doxorubicin (DOX) release (Scheme 1). PEG-AAPU(SS)-PEG copolymers could be readily obtained *via* polycondensation reaction between two α-amino acid derivatives, disulfide-linked bis(ethyl L-serinate) (SS-BSER) and L-lysine ethyl ester diisocyanate (LDI), followed by reacting with mPEG-NCO. LDI derived from L-lysine is a biocompatible diisocyanate. To the best of our knowledge, this is the first report on the development of α-amino acid-based poly(disulfide urethane)s and the corresponding triblock copolymer micelles.

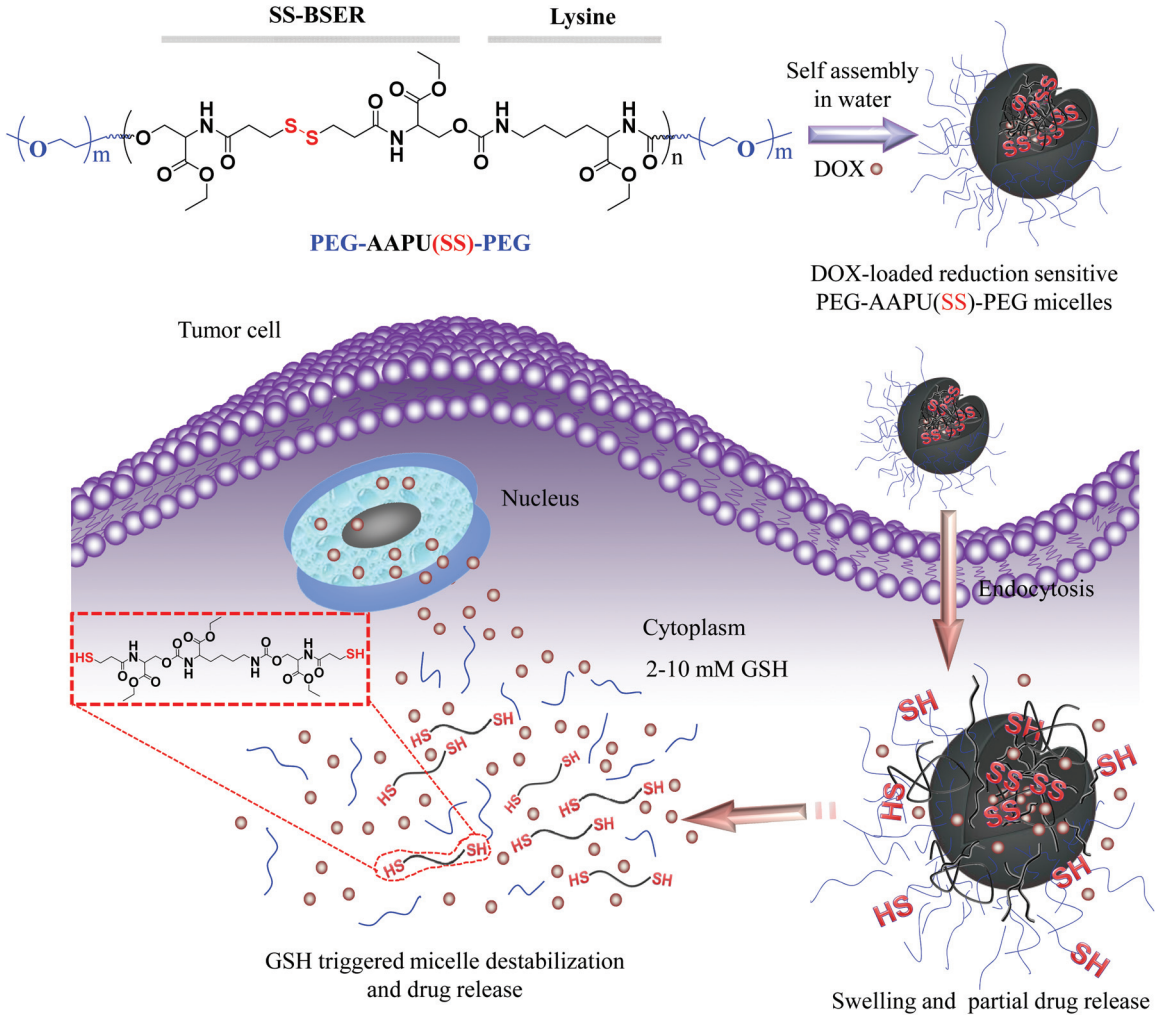

Scheme 1 Illustration of PEG-AAPU(SS)-PEG triblock copolymer micelles for triggered intracellular DOX release.

Experimental section

Materials

3,3′-Dithiodipropionic acid (DTDPA, 99%, Alfa Aesar), ethyl L-serinate hydrochloride (SER, 98%, Alfa Aesar), *N*-hydroxysuccin imide (NHS, 98%, Alfa Aesar), 1-(3-dimethylaminopropyl)-3-ethylcarbodiimide hydrochloride (EDC, 98%, Alfa Aesar), dibutyltin dilaurate (DBTDL, 97.5%, J&K), L-lysine ethyl ester dihydrochloride (LEED, 98%, J&K), glutathione (GSH, 99%, Roche), DL-1,4-dithiothreitol (DTT, 99%, J&K), *N*,*N*-dimethylformamide (DMF, 99%, Alfa Aesar), and 3-(4,5-dimethylthiazol-2-yl)-2,5-diphenyltetrazoliumbromide (MTT) were used as received. Doxorubicin hydrochloride (DOX·HCl, 99%, Beijing ZhongShuo Pharmaceutical Technology Development Co., Ltd) was pretreated with triethylamine to detach hydrochloride. Methoxy poly(ethylene glycol) (mPEG-OH, M_n = 5.0 kg mol^{-1}, Fluka) was dried by azeotropic distillation from anhydrous toluene. Dichloromethane (DCM) was dried by refluxing over CaH_2 under an argon atmosphere. Triphosgene (BTC, Shanxi Jiaocheng Jingxin Chemical Factory) was recrystallized with ethyl acetate prior to use. mPEG-NCO was synthesized as per previous reports.[40,41]

Measurements

^{1}H NMR spectra were recorded on a Unity Inova 400 spectrometer operating at 400 MHz using DMSO-d_6 or $CDCl_3$ as a solvent. The chemical shifts were calibrated against solvent residue signals. Elemental analyses were performed on a Perkin-Elmer EA 240. Fourier transform infrared spectrometry (Varian 3600 FTIR) was performed on a thermo scientific spectrophotometer with Omnic software for data acquisition and analysis. Polymers were ground into KBr powder and pressed into discs prior to FTIR analysis. The molecular weight and polydispersity of polymers were determined by a Waters 1515 gel permeation chromatograph (GPC) equipped with MZ-gel SD plus columns (500 Å, 10^3 Å, 10^4 Å) following a differential refractive-index detector (RID 2414). The measurements were performed using DMF containing 0.05 mol L^{-1} LiBr as the eluent at a flow rate of 0.8 mL min^{-1} at 40 °C. A series of narrow PMMA standards were used for calibration. Thermal properties of AAPU(SS)s were characterized using a differential scanning calorimeter (DSC, TA Q200). The measurements were carried out from −80 to 120 °C at a heating rate of 20 °C min^{-1} under a 25 mL min^{-1} nitrogen flow. TA Universal Analysis software was used for thermal data analysis of glass transition temperature (T_g). The size of micelles was determined using dynamic light scattering (DLS). Measurements were carried out at 25 °C by using a Zetasizer Nano-ZS from Malvern Instruments equipped with a 633 nm He–Ne laser using back-scattering detection. Fluorescence spectra were recorded using a FLS920 fluorescence spectrometer. Transmission electron microscopy (TEM) was performed using a Tecnai G220 TEM operated at an accelerating voltage of 120 kV. The samples were prepared by dropping 10 μL of 0.5 mg mL^{-1} micelles dispersion on the copper grid followed by staining with 1 wt% phosphotungstic acid. The fluorescence images were taken on a confocal laser scanning microscope (TCS SP5).

Synthesis of SS-BSER

SS-BSER was synthesized from an amidation reaction between DTDPA and SER in water by EDC/NHS chemistry (Scheme S1†). In brief, DTDPA (4.20 g, 20 mmol), EDC (11.46 g, 60 mmol) and NHS (6.90 g, 60 mmol) were dissolved in H_2O (100 mL) at room temperature. The reaction mixture was stirred for 12 h and SER (10.14 g, 60 mmol) was added. The reaction was allowed to proceed at pH 8.0 for additional 24 h at room temperature. The reaction mixture was extracted with DCM, the organic phase was collected and dried over anhydrous $MgSO_4$, the solvent was removed, and the product following purification by recrystallization in THF and diethyl ether was dried *in vacuo* for 2 days. Yield: 45.8%. ^{1}H NMR (400 MHz, DMSO-d_6): δ (ppm): 8.29 (d, 2H, –CH–*NH*–CO–), 5.02 (t, 2H, –CH_2–*OH*), 4.32 (t, 2H, –CH_2–*CH*–COO–), 4.09 (m, 4H, –COO–*CH_2*–CH_3), 3.66 (m, 4H, –*CH_2*–OH), 2.89 (t, 4H, –CH_2–*CH_2*–SS–), 2.57 (t, 4H, –CO–*CH_2*–CH_2–), 1.19 (t, 6H, –CH_2–*CH_3*). Elemental analysis for SS-BSER ($C_{16}H_{28}O_8N_2S_2$) (%): C, 43.32; H, 6.42; N, 6.24. Found: C, 43.63; H, 6.36; N, 6.36. Electrospray ionization mass spectrometry (ESI-MS, *m*/*z*): calcd for $C_{16}H_{28}O_8N_2S_2$ 440.0; found 440.0.

Synthesis of AAPU(SS)s

AAPU(SS)s were prepared by the polycondensation reaction between SS-BSER and LDI in DMF using DBTDL as a catalyst. Taking the synthesis of AAPU(SS)-2 as an example, under a N_2 atmosphere, to a solution of LDI (0.226 g, 1.0 mmol) and a catalytic amount of DBTDL (6.84 mg, 10 μmol) in DMF (4 mL) was added SS-BSER (0.458 g, 1.04 mmol) under stirring. The polymerization reaction was allowed to proceed at 60 °C for 24 h. The resulting polymer was isolated by precipitating in cold diethyl ether and dried *in vacuo* at room temperature. Yield: 91.8%. ^{1}H NMR (400 MHz, DMSO-d_6): δ 4.50, 4.22, 4.09, 3.92, 3.66, 2.89, 2.57 and 1.19–1.59.

Reductive degradation of AAPU(SS)s

Under a N_2 atmosphere, 10 mg of AAPU(SS)-2 was dissolved in 2 mL of DMF containing 200 mM DTT. The solution was stirred at 37 °C for 4 h. The degradation product was recovered by precipitation in 20-fold excess water and further washed three times with water and two times with diethyl ether. The molecular weight of degradation products was measured by GPC.

Synthesis of the PEG-AAPU(SS)-PEG triblock copolymer

PEG-AAPU(SS)-PEG triblock copolymer was prepared by a coupling reaction between mPEG-NCO and AAPU(SS)-2. Briefly, to a solution of AAPU(SS)-2 (0.40 g, 30 μmol) in DMF (5 mL) at 65 °C were added mPEG-NCO (0.90 g, 0.18 mmol) and a catalytic amount of DBTDL (13.0 mg, 20 μmol). The reaction was allowed to proceed with stirring at 65 °C for 24 h. The resulting copolymer was isolated by twice precipitation from a mixture of diethyl ether and methanol, filtration and drying *in vacuo* at

room temperature. Yield: 64.7%. ^{1}H NMR (400 MHz, DMSO-d_6): PEG block: δ 3.51 and 3.24; AAPU(SS) block: δ 4.50, 4.22, 4.09, 3.92, 3.66, 2.89, 2.57 and 1.19–1.59.

Micelle formation and critical micelle concentration (CMC)

Micelles were typically prepared by dropwise addition of 0.8 mL of phosphate buffer (PB, 10 mM, pH 7.4) into 0.2 mL of the PEG-AAPU(SS)-PEG triblock copolymer solution in DMF (5.0 wt%) under stirring at room temperature followed by extensive dialysis against PB (10 mM, pH 7.4) (MWCO 3500).

Pyrene was used as a fluorescence probe for the CMC determination. The concentration of the PEG-AAPU(SS)-PEG triblock copolymer varied from 2.0×10^{-5} to 0.2 mg mL^{-1} and the concentration of pyrene was fixed at 1.0 μM. Fluorescence spectra were recorded at an excitation wavelength of 330 nm. Fluorescence emissions at 372 and 383 nm were monitored. The CMC was estimated as the cross-point when extrapolating the intensity ratio I_{372}/I_{383} at low and high concentration regions.

Change of PEG-AAPU(SS)-PEG micelle sizes in response to 10 mM GSH

Under a N_2 atmosphere, 2.0 mL of PEG-AAPU(SS)-PEG micelle dispersion (1 mg mL^{-1}) was divided into two aliquots, one in PB (10 mM, pH 7.4) and the other in PB (10 mM, pH 7.4) containing 10 mM GSH. The dispersions were gently stirred at 37 °C. Micelle sizes and count rates were monitored at different time intervals by DLS.

Loading and reduction-triggered release of DOX

DOX-loaded micelles were prepared by dropwise addition of PB (10 mM, pH 7.4, 0.8 mL) to a mixture of copolymer solution in DMF (5.0 mg mL^{-1}, 0.2 mL) and DOX solution in DMSO (5.0 mg mL^{-1}, 10, 20, or 40 μL) under stirring at room temperature, followed by dialysis against PB (10 mM, pH 7.4) in the dark for 7 h (MWCO 3500). The dialysis media were changed five times.

To determine the drug loading content (DLC), 100 μL of DOX-loaded micelle dispersion was freeze-dried, dissolved in 3 mL of DMSO and analyzed with fluorescence spectroscopy. A calibration curve was obtained using DOX/DMSO solutions with different DOX concentrations. To determine the amount of DOX released, calibration curves were run with DOX/corresponding buffer solutions with different DOX concentrations. The emission at 560 nm was recorded. The DLC and drug loading efficiency (DLE) were calculated according to the following formula:

$$\mathrm{DLC(wt\%)} = (\text{weight of loaded drug/totalweight of loaded drug and polymer}) \times 100$$

$$\mathrm{DLE\ (\%)} = (\text{weight of loaded drug/weight of drug in feed}) \times 100$$

The *in vitro* release of DOX from DOX-loaded PEG-AAPU(SS)-PEG micelles was investigated at 37 °C under two different conditions, *i.e.* (i) PB (10 mM, pH 7.4), and (ii) PB (10 mM, pH 7.4) with 10 mM GSH. In order to acquire the sink conditions, drug release studies were performed at a low DLC of 2.5 wt% and with 0.5 mL of micelle dispersion dialysis against 25 mL of appropriate medium (MWCO 12 000–14 000). At desired time intervals, 5.0 mL of the release media was taken out and refreshed with an equal volume of fresh medium. To minimize oxidation of GSH, the release studied were carried out under a N_2 atmosphere. The amount of DOX released was determined by fluorescence measurements (excitation at 488 nm, emission at 560 nm). The release experiments were conducted in triplicate. The results presented are the average data.

MTT assays

The cytotoxicity of PEG-AAPU(SS)-PEG micelles was determined using DOX-resistant MCF-7 human breast cancer cells (MCF-7/ADR) and mouse leukaemic monocyte macrophage cells (RAW 264.7). DOX-loaded micelles at a drug loading content (DLC) of 7.5 wt% were used. MCF-7/ADR cells were plated in a 96-well plate (1×10^4 cells per well) in RPMI 1640 media supplemented with 10% fetal bovine serum (FBS), 1% L-glutamine, and antibiotics penicillin (100 IU mL^{-1}) and streptomycin (100 μg mL^{-1}). After 24 h, the medium was removed and replenished by 80 μL of fresh medium. 20 μL of blank PEG-AAPU(SS)-PEG micelles was added leading to final micelle concentrations of 0.1, 0.2, 0.4, 0.8 and 1.0 mg mL^{-1}, respectively. The cells were incubated under 5% CO_2 atmosphere for 48 h at 37 °C. The medium was aspirated and replaced with 100 μL of fresh medium. 10 μL of 3-(4,5-dimethylthiazol-2-yl)-2,5-diphenyltetrazolium bromide (MTT) solution (5 mg mL^{-1}) was added. The cells were incubated for another 4 h. The medium was carefully aspirated, MTT-formazan generated by live cells was dissolved in 150 μL of DMSO, and the absorbance at a wavelength of 570 nm of each well was measured using a microplate reader (Bio-Tek, ELX808IU). The relative cell viability (%) was determined by comparing the absorbance at 570 nm with control wells containing only cell culture medium. MTT assays in RAW 264.7 cells were performed in a similar way except that Dulbecco's Modified Eagle's Medium (DMEM) containing 10% FBS, 1% L-glutamine, and antibiotics penicillin (100 IU mL^{-1}) and streptomycin (100 μg mL^{-1}) was used.

The antitumor activity of DOX-loaded PEG-AAPU(SS)-PEG micelles and free DOX·HCl was also studied by MTT assays. MCF-7/ADR cells were plated in a 96-well plate (1×10^4 cells per well) in RPMI 1640 media supplemented with 10% fetal bovine serum (FBS), 1% L-glutamine, and antibiotics penicillin (100 IU mL^{-1}) and streptomycin (100 μg mL^{-1}). After 24 h, the medium was removed and replenished by 80 μL of fresh medium. 20 μL of DOX-loaded PEG-AAPU(SS)-PEG micelles or free DOX·HCl was added resulting in a final DOX concentrations of 10, 20 and 40 μg mL^{-1}, respectively. The cells were incubated under 5% CO_2 atmosphere for 48 h at 37 °C. The medium was aspirated and replaced with 100 μL of fresh medium. 10 μL of MTT solution (5 mg mL^{-1}) was added and the cells were incubated for another 4 h. The medium was

aspirated, the MTT-formazan generated by live cells was dissolved in 150 μL of DMSO, and the absorbance at a wavelength of 570 nm of each well was measured using a microplate reader. The cell viabilities were determined by MTT assays as described above. For RAW 264.7 cells, DMEM containing 10% FBS, 1% L-glutamine, and antibiotics penicillin (100 IU mL^{-1}) and streptomycin (100 μg mL^{-1}) was used as a culture medium and DOX concentrations varied from 0.001, 0.01, 0.1, 1, 5, 10, 20 to 40 μg mL^{-1}.

Confocal laser scanning microscopy (CLSM) measurements

The cellular uptake and intracellular release behaviors of DOX-loaded PEG-AAPU(SS)-PEG micelles were followed by CLSM using MCF-7/ADR cells. DOX-loaded micelles at a DLC of 7.5 wt% were used. MCF-7/ADR cells were plated in a 24-well plate (5×10^4 cells per well) in RPMI 1640 media supplemented with 10% FBS, 1% L-glutamine, and antibiotics penicillin (100 IU mL^{-1}) and streptomycin (100 μg mL^{-1}) for 24 h. The media were aspirated and replaced with 450 μL of fresh medium. 50 μL of DOX-loaded micelles or free DOX·HCl (drug dosage: 20.0 μg mL^{-1}) was added. The cells were incubated at 37 °C for 4 or 8 h with DOX-loaded micelles or 4 h with free DOX·HCl under a humidified 5% CO_2 atmosphere. The culture medium was removed and the cells were rinsed three times with phosphate buffered saline (PBS, pH 7.4, 10 mM). The cells were fixed with 4% paraformaldehyde for 20 min and washed with PBS three times. The cell nuclei were stained with 4,6-diamidino-2-phenylindole (DAPI, blue) for 20 min and washed with PBS three times. Fluorescence images of the cells were obtained with a confocal laser scanning microscope (TCS SP5).

Flow cytometry analysis

MCF-7/ADR cells were seeded onto 6-well plates at 1×10^5 cells per well (1 mL) for 24 h. DOX-loaded micelles at a DLC of 7.5 wt% were used. DOX-loaded micelles and free DOX·HCl were added (drug dosage: 10.0 μg mL^{-1}). After incubation at 37 °C for 4 or 8 h, the cells were digested by 0.25% w/v trypsin/0.03% w/v EDTA. The suspensions were centrifuged at 1000 rpm for 4 min at 4 °C, pelleted in Eppendorf tubes, washed twice with cold PBS, and then resuspended in 500 μL of PBS with 2% FBS. Fluorescence histograms were recorded with a BD FACSCalibur (Becton Dickinson) flow cytometer and analyzed using Cell Quest software. We analyzed 10 000 gated events to generate each histogram. The gate was arbitrarily set for the detection of red fluorescence.

Results and discussion

Synthesis of AAPU(SS)s

AAPU(SS)s were synthesized *via* polycondensation reaction between two α-amino acid derivatives, disulfide-linked bis-(ethyl L-serinate) (SS-BSER) and L-lysine ethyl ester diisocyanate (LDI) (Scheme 2). SS-BSER was prepared by reaction of DTDPA with excess SER through carbodiimide chemistry and purified by recrystallization from THF and diethyl ether (Scheme S1†). ^{1}H NMR also displayed in addition to resonances owing to SER moieties (δ 1.19, 3.66, 4.09, 4.32 and 5.02) and DTDPA moieties (δ 2.57 and 2.89) a new signal attributable to the amide proton at δ 8.29 (Fig. 1A). The signals at δ 1.19 (methyl protons of SER) and δ 2.57 (methylene protons next to the carbonyl group in DTDPA) had an integral ratio close to 3 : 2, supporting quantitative conjugation of DTDPA with SER. ^{13}C NMR revealed two resonances at δ 171.0 and 170.8 (Fig. 1B), which were attributable to the carbonyl carbon of amide and ester

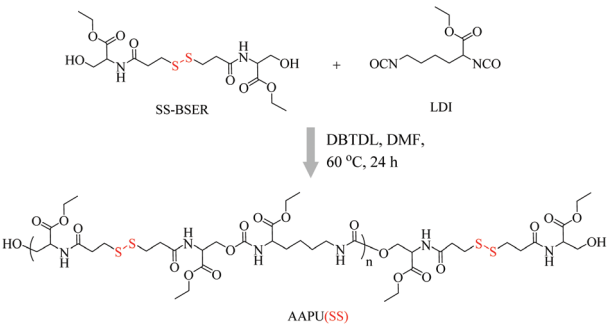

Scheme 2 Synthesis of AAPU(SS)s.

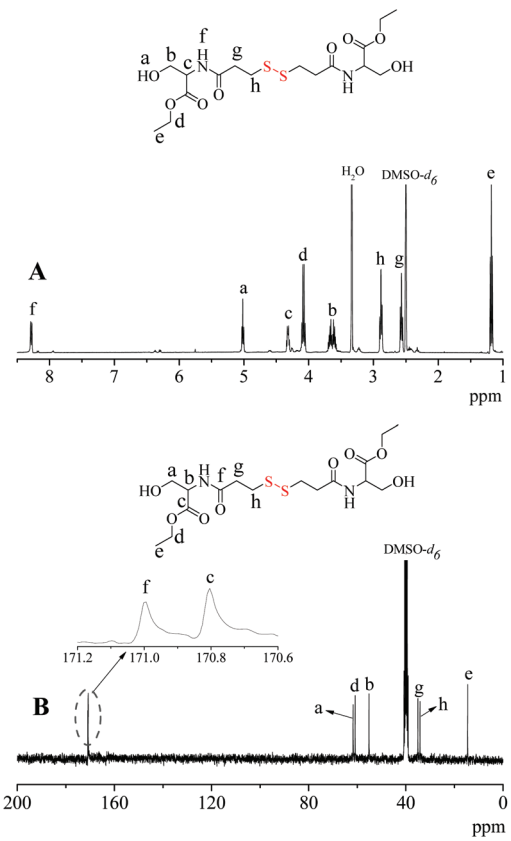

Fig. 1 (A) ^{1}H NMR (400 MHz, DMSO-d_6) and (B) ^{13}C NMR (75 MHz, DMSO-d_6) spectra of SS-BSER.

bonds, respectively. The structure of SS-BSER has further been confirmed by elemental analysis and mass spectrum.

The polycondensation reaction between SS-BSER and LDI was carried out in DMF at 60 °C using DBTDL as a catalyst at different SS-BSER/LDI molar feed ratios of 1.08/1, 1.04/1, 1.02/1 and 1.01/1. The extent of polymerization was monitored by FTIR. The results revealed the disappearance of the characteristic absorbance of isocyanate in 24 h at 2300–2250 cm^{-1} (Fig. S1†), indicating complete polycondensation. Table 1 summarizes the polymerization results. ^{1}H NMR showed signals assignable to LDI moieties (δ 1.19–1.59, 2.89, 3.92 and 4.09) and SS-BSER moieties (δ 1.19, 2.57, 2.89, 3.66, 4.09, 4.22 and 4.50), respectively (Fig. 2). The SS-BSER/LDI molar ratios in AAPU(SS)s determined by comparing the integrals of signals at δ 3.92 and δ 4.50 were in parallel with the molar feed ratios (Table 1). As SS-BSER was excess in feed and polycondensation went to completion, AAPU(SS)s were obtained with the hydroxyl groups at both ends. The signal assignable to the methylene protons neighboring the hydroxyl end groups of AAPU(SS) was clearly detected at δ 3.66 (Fig. 2). ^{1}H NMR end group analysis showed that AAPU(SS)s had M_n varying from 4.6 to 35.7 kg mol^{-1}, which increased with decreasing SS-BSER/LDI molar feed ratios from 1.08/1 to 1.01/1 (Table 1). GPC displayed that AAPU(SS)s had a unimodal distribution with a moderate PDI of 1.5–1.9 and M_n values ranging from 9.1 to 88.9 kg mol^{-1} depending on SS-BSER/LDI molar feed ratios. The deviation in M_n (GPC) from M_n (^{1}H NMR) is likely due to the fact that PMMA was used to calibrate the GPC columns. In spite of differences in M_n values, M_n determined by GPC increased in good accordance with that determined by ^{1}H NMR end group analyses and close to those (M_n ranging from 9.4 to 67.0 kg mol^{-1}) calculated based on the Carothers equation assuming 100% conversion of NCO. Thermal analyses indicated that the thus obtained AAPU(SS)s were amorphous with T_g ranging from 31.7 to 49.2 °C (Fig. 3), which increased with increasing M_n. Notably, these α-amino acid-based PUs had much higher T_g than those based on PCL or PEO.[42,43] In order to verify their reductive degradation properties, AAPU(SS) following incubation with 200 mM DTT in DMF for 4 h was subjected to GPC measurements. The results showed that M_n of AAPU(SS) declined from 25.1 to 0.85 kg mol^{-1}, corroborating fast and complete cleavage of the disulfide bonds in the backbone (Fig. S2†).

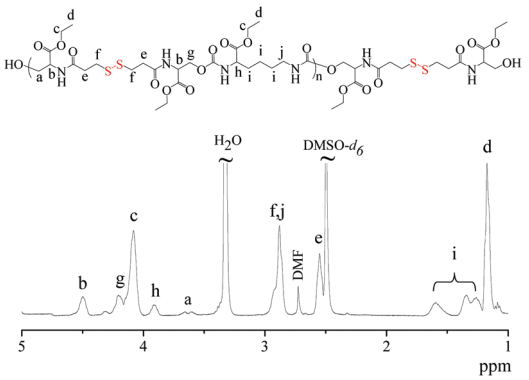

Fig. 2 ^{1}H NMR spectrum (400 MHz, DMSO-d_6) of AAPU(SS)-2.

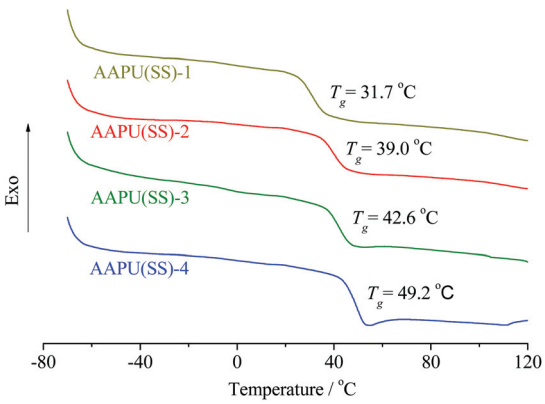

Fig. 3 DSC curves of AAPU(SS)s.

Synthesis of PEG-AAPU(SS)-PEG

AAPU(SS)-2 with an M_n of 12.3 kg mol^{-1} and a PDI of 1.5 was chosen to prepare a PEG-AAPU(SS)-PEG triblock copolymer. PEG-AAPU(SS)-PEG was obtained by reacting AAPU(SS) with 6-fold mPEG-NCO (M_n = 5.0 kg mol^{-1}) in DMF at 65 °C in the presence of a catalytic amount of DBTDL for 24 h (Scheme 3). The excess PEG was removed by precipitation in a diethyl ether/methanol mixture. ^{1}H NMR discerned signals assignable to the methoxy and methylene protons of mPEG (δ 3.24 and 3.51) but no peaks at δ 3.66 ascribable to the methylene

Table 1 Synthesis of AAPU(SS)s

	SS-BSER/LDI molar ratio		M_n (kg mol^{-1})				
Prepolymer	In feed	^{1}H NMR[a]	^{1}H NMR[a]	GPC[b]	PDI[b]	T_g[c] (°C)	Yield (%)
AAPU(SS)-1	1.08/1	1.16/1	4.6	9.1	1.6	31.7	84.3
AAPU(SS)-2	1.04/1	1.06/1	12.3	25.1	1.5	39.0	91.8
AAPU(SS)-3	1.02/1	1.03/1	20.6	47.8	1.9	42.6	93.4
AAPU(SS)-4	1.01/1	1.02/1	35.7	88.9	1.6	49.2	95.8

[a] Determined by ^{1}H NMR. [b] Determined by GPC measurements using DMF as an eluent at a flow rate of 0.8 mL min^{-1} (standards: PMMA, 40 °C). [c] T_g (glass transition temperature) determined by DSC (heating from −80 °C to 120 °C at a rate of 20 °C min^{-1}).

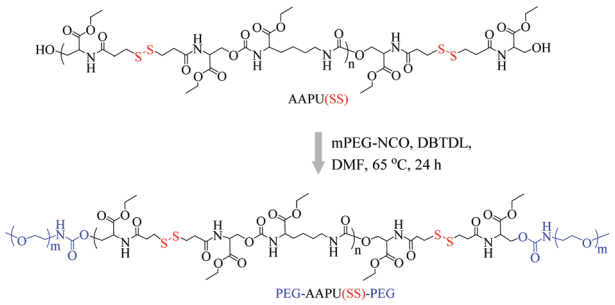

Scheme 3 Synthesis of the PEG-AAPU(SS)-PEG triblock copolymer.

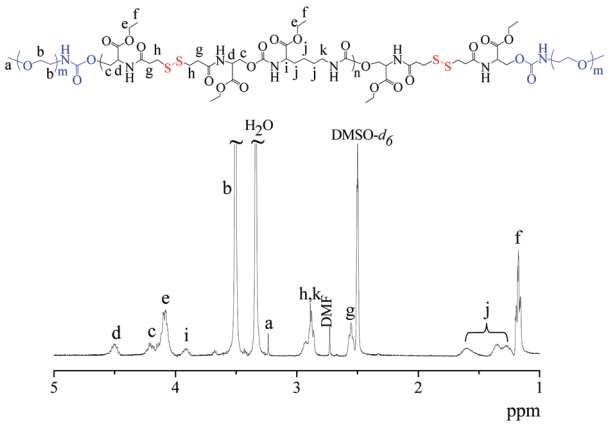

Fig. 4 ^{1}H NMR spectrum (400 MHz, DMSO-d_6) of the PEG-AAPU(SS)-PEG triblock copolymer.

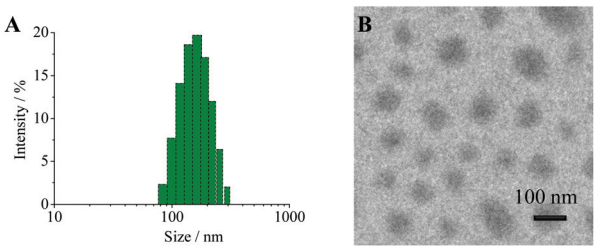

Fig. 5 Size distribution of PEG-AAPU(SS)-PEG micelles determined by (A) DLS and (B)TEM.

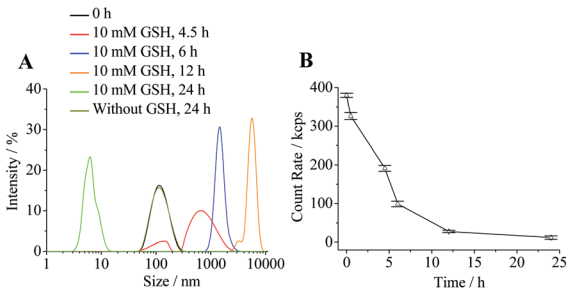

Fig. 6 Change of (A) size distribution and (B) count rates of PEG-AAPU(SS)-PEG micelles studied by DLS in PB (10 mM, pH 7.4) either in the presence or absence of 10 mM GSH at 37 °C.

protons next to the hydroxyl end groups in the AAPU(SS) prepolymer (Fig. 4), indicating successful conjugation of PEG to both sides of AAPU(SS). The intensity comparison of signals at δ 3.92 (methine protons in LDI moieties of AAPU(SS) block) and 3.51 (methylene protons of PEG) confirmed that two PEG chains were coupled to one AAPU(SS). Moreover, the GPC curve showed that PEG-AAPU(SS)-PEG had a unimodal distribution with a low PDI of 1.3, which was lower than the corresponding AAPU(SS) (Fig. S3†). These results demonstrated the successful synthesis of the PEG-AAPU(SS)-PEG triblock copolymer.

Formation and reduction triggered dissociation of PEG-AAPU(SS)-PEG micelles

PEG-AAPU(SS)-PEG triblock copolymer micelles were prepared by the solvent exchange method. As shown by dynamic light scattering (DLS), PEG-AAPU(SS)-PEG formed nanosized micelles with an average diameter of *ca.* 155 nm and a low polydispersity of 0.17 in PB (10 mM, pH 7.4) (Fig. 5A). TEM revealed that PEG-AAPU(SS)-PEG micelles had a mean diameter of *ca.* 100 nm (Fig. 5B), which was smaller than that determined by DLS likely due to micelle shrinkage upon dying. The critical micelle concentration (CMC) determined using pyrene as a probe revealed that PEG-AAPU(SS)-PEG had a low CMC of 3.31 mg L^{-1} in 10 mM PB at pH 7.4.

The *in vitro* stability and reduction-responsivity of PEG-AAPU(SS)-PEG micelles were studied by DLS in PB (10 mM, pH 7.4) at 37 °C. Notably, under a non-reductive condition, no change in micelle size distribution was discerned in 24 h (Fig. 6A), implying that PEG-AAPU(SS)-PEG micelles have adequate aqueous stability. In contrast, under an intracellular mimicking reductive environment containing 10 mM GSH, micelles underwent rapid swelling to over 1000 nm in 6 h and turned into about 4 nm in 24 h (Fig. 6A), indicating complete disruption of micelles. In accordance, a fast decrease in the count rates was observed in the presence of 10 mM GSH (Fig. 6B). These results corroborate fast responsivity of PEG-AAPU(SS)-PEG micelles to cytoplasmic reductive conditions, similar to our previous report for reductively degradable SS-PEA nanoparticles.[31]

Loading and triggered release of DOX

DOX-loaded micelles were prepared through a solvent exchange method. DOX was loaded in a desalted form into PEG-AAPU(SS)-PEG micelles at theoretical DLCs of 5, 10, and 20 wt%. The results showed that DLE ranging from 40.5 to 50.5% and a decent DLC of 7.5 wt% could be achieved (Table 2). The sizes of DOX-loaded PEG-AAPU(SS)-PEG micelles increased from 158 to 180 nm with increasing DLCs from 2.5 to 7.5 wt%. The *in vitro* drug release studies were carried out at

Table 2 Characteristics of DOX-loaded PEG-AAPU(SS)-PEG micelles

Entry	DLC (theo) (wt%)	Micelles Size[a] (nm)	PDI[a]	DLC[b] (wt%)	DLE[b] (%)
1	5	158	0.08	2.5	50.5
2	10	164	0.13	4.2	43.8
3	20	180	0.17	7.5	40.5

[a] Determined by DLS at 25 °C in PB (10 mM, pH 7.4). [b] Determined by fluorescence measurements.

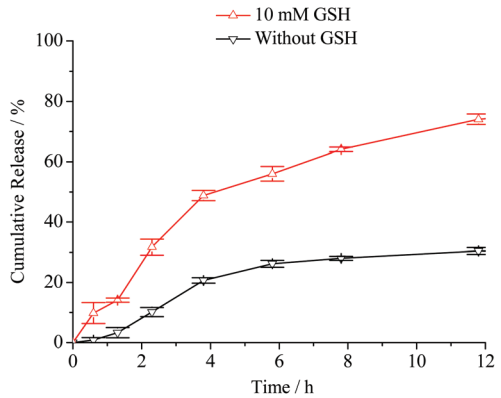

Fig. 7 GSH-triggered release of DOX from DOX-loaded PEG-AAPU(SS)-PEG micelles in PB (pH 7.4, 10 mM). The drug release studies were performed at a low micelle concentration of 0.2 mg mL^{-1} and a low drug loading content of 5 wt%. Data are presented as mean ± SD (n = 3).

a low micelle concentration of 0.2 mg mL^{-1} at 37 °C using a dialysis tube (MWCO 12 000) in PB buffer (pH 7.4) either in the presence or absence of 10 mM GSH. Fig. 7 shows that DOX was quickly released in response to 10 mM GSH wherein *ca.* 49% and 74% of DOX were released in 4 and 12 h, respectively. In contrast, only 29% of the drug was released within 12 h in the absence of 10 mM GSH under the otherwise same conditions. This reduction-triggered drug release behavior renders PEG-AAPU(SS)-PEG micelles interesting for cytoplasmic anticancer drug delivery into cancer cells.

MTT, confocal microscopy and flow cytometry studies in RAW 264.7 and MCF-7/ADR cells

The cytotoxicity of PEG-AAPU(SS)-PEG micelles and antitumor activity of DOX-loaded PEG-AAPU(SS)-PEG micelles were evaluated by MTT assays in RAW 264.7 and MCF-7/ADR cells. The results revealed that PEG-AAPU(SS)-PEG micelles were non-cytotoxic even at a high concentration of 1.0 mg mL^{-1} (Fig. 8), confirming that α-amino acid-based poly(disulfide urethane)s have good biocompatibility. In contrast, DOX-loaded PEG-AAPU(SS)-PEG micelles caused effective growth inhibition of both RAW 264.7 and MCF-7/ADR cells (Fig. 9). The half-maximal inhibitory concentration (IC_{50}) was 10.0 μg DOX equiv. per mL in RAW 264.7 cells (Fig. 9A), which was higher

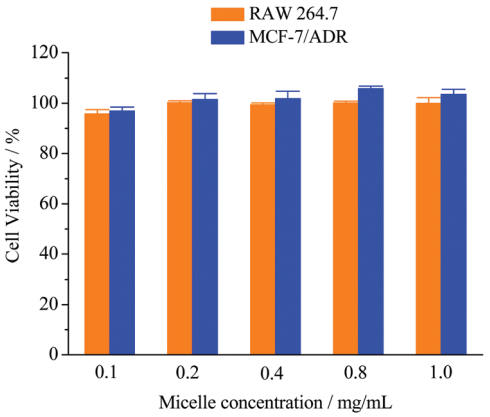

Fig. 8 MTT assays of blank PEG-AAPU(SS)-PEG micelles in RAW 264.7 and MCF-7/ADR cells. The cells were incubated with micelles for 48 h. Results are presented as the mean ± SD (n = 4).

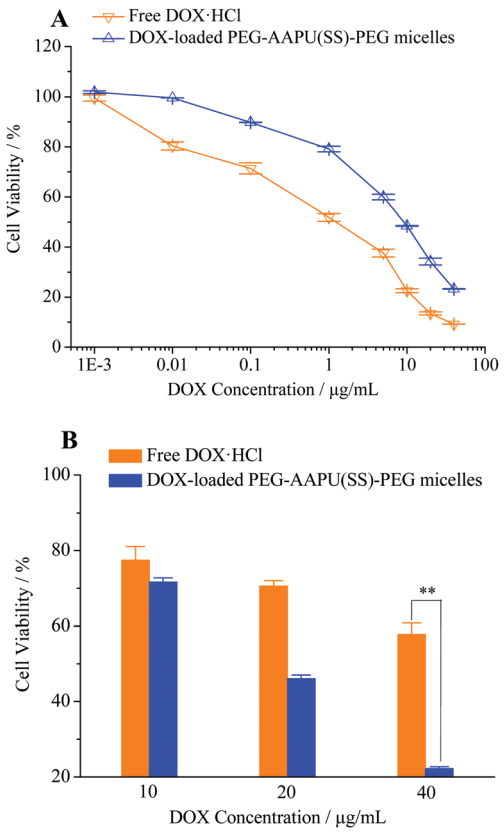

Fig. 9 MTT assays of DOX-loaded PEG-AAPU(SS)-PEG micelles and free DOX·HCl in RAW 264.7 cells (A) and MCF-7/ADR cells (B) following 48 h incubation. Results are presented as the mean ± SD (n = 4). (Student's t-test, $^{**}p < 0.01$).

than free DOX·HCl (IC_{50} = 1.0 μg mL^{-1}). The reduced toxicity of DOX-loaded PEG-AAPU(SS)-PEG micelles is likely due to the presence of effective PEG stealth and inefficient cellular uptake.

Notably, DOX-loaded PEG-AAPU(SS)-PEG micelles were significantly more potent than free DOX·HCl against drug resistant MCF-7/ADR cells, in which cell viabilities of 22.3% and 57.9% were observed for DOX-loaded PEG-AAPU(SS)-PEG micelles and free DOX·HCl, respectively, at a DOX dosage of 40 μg mL^{-1} (Fig. 9B). This effective reversal of drug resistance is most probably due to a combination of cellular uptake *via* the endocytosis mechanism and triggered intracellular drug release.[44,45] CLSM was employed to study the intracellular DOX release from PEG-AAPU(SS)-PEG micelles in MCF-7/ADR cells. As shown in Fig. 10, strong DOX fluorescence was detected in the cytoplasm and perinuclear regions of MCF-7/ADR cells following 4 and 8 h incubation, corroborating a high intracellular free DOX level. This high DOX concentration in MCF-7/ADR cells most likely resulted from rapid intracellular DOX release. In contrast, little DOX fluorescence was observed in MCF-7/ADR cells following 4 h treatment with free DOX·HCl. The high intracellular DOX level in MCF-7/ADR cells treated with DOX-loaded PEG-AAPU(SS)-PEG micelles has further been confirmed by flow cytometry analyses (Fig. S4†). These results indicate that PEG-AAPU(SS)-PEG micelles offer a particularly interesting platform for targeted tumor chemotherapy, wherein the cell uptake and antitumor activity of PEG-AAPU(SS)-PEG micelles could be modulated by installing a specific targeting ligand.

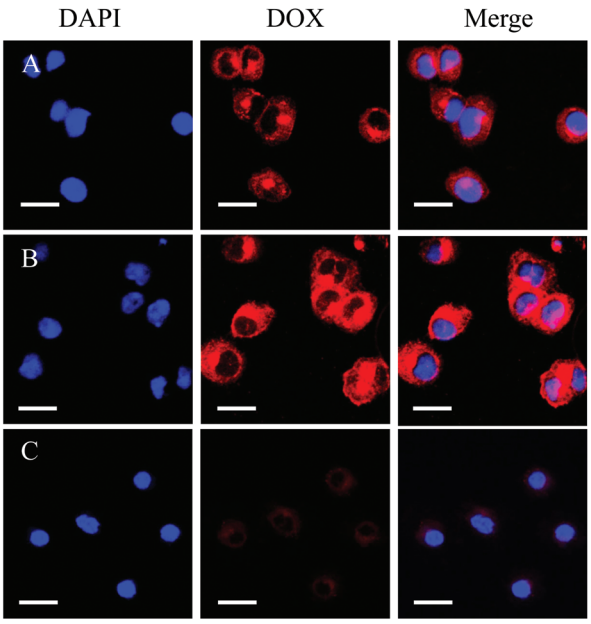

Fig. 10 CLSM images of MCF-7/ADR cells following incubation with DOX-loaded PEG-AAPU(SS)-PEG micelles or free DOX·HCl (dosage: 20 μg DOX equiv. per mL). (A) DOX-loaded PEG-AAPU(SS)-PEG micelles, 4 h incubation; (B) DOX-loaded PEG-AAPU(SS)-PEG micelles, 8 h incubation; and (C) free DOX·HCl, 4 h incubation. For each panel, the images show cell nuclei stained with DAPI (blue), DOX fluorescence in cells (red), and overlays of the two images. The scale bars correspond to 20 μm in all the images.

Conclusions

In this paper, we have developed novel α-amino acid-based biocompatible and bioreducible poly(disulfide urethane)s as well as corresponding triblock copolymer micelles for triggered intracellular drug release. AAPU(SS) can be readily prepared with controlled molecular weights under mild conditions. PEG-AAPU(SS)-PEG micelles offer several unique merits: (i) they are mainly based on α-amino acids, endowing superior biocompatibility, which is of critical importance for biomedical applications; (ii) they exhibit fast GSH-triggered drug release behavior, resulting in efficient cytoplasmic anticancer drug delivery and high antitumor efficacy; and (iii) they are easy to prepare with controlled structures and molecular weights. These amino acid-based biocompatible and bioreducible polymeric micelles have appeared to be an appealing platform for triggered intracellular anticancer drug delivery.

Acknowledgements

This work was supported by the National Natural Science Foundation of China (NSFC 51103093 and 51373113), the National Science Fund for Distinguished Young Scholars (51225302), the Natural Science Foundation of Jiangsu Province (BK20131166), a Project Funded by the Priority Academic Program Development of Jiangsu Higher Education Institutions and the Project of Science and Technology of Suzhou (SYG201331).

Notes and references

1 T. J. Deming, *Prog. Polym. Sci.*, 2007, **32**, 858–875.
2 D. W. Löwik, E. Leunissen, M. Van den Heuvel, M. Hansen and J. C. van Hest, *Chem. Soc. Rev.*, 2010, **39**, 3394–3412.
3 C. Deng, J. Wu, R. Cheng, F. Meng, H.-A. Klok and Z. Zhong, *Prog. Polym. Sci.*, 2014, **39**, 330–364.
4 H. Sun, F. Meng, A. A. Dias, M. Hendriks, J. Feijen and Z. Zhong, *Biomacromolecules*, 2011, **12**, 1937–1955.
5 Y. Feng, J. Lu, M. Behl and A. Lendlein, *Macromol. Biosci.*, 2010, **10**, 1008–1021.
6 R. A. Perez, J.-E. Won, J. C. Knowles and H.-W. Kim, *Adv. Drug Delivery Rev.*, 2013, **65**, 471–496.
7 S. Pascual-Gil, E. Garbayo, P. Díaz-Herráez, F. Prosper and M. J. Blanco-Prieto, *J. Controlled Release*, 2015, **203**, 23–38.
8 Q. Chen, S. Liang and G. A. Thouas, *Prog. Polym. Sci.*, 2013, **38**, 584–671.
9 M. Kütting, J. Roggenkamp, U. Urban, T. Schmitz-Rode and U. Steinseifer, *Expert. Rev. Med. Devices*, 2011, **8**, 227–233.
10 P. Singhal, W. Small, E. Cosgriff-Hernandez, D. J. Maitland and T. S. Wilson, *Acta Biomater.*, 2014, **10**, 67–76.
11 R. J. Zdrahala and I. J. Zdrahala, *J. Biomater. Appl.*, 1999, **14**, 67–90.
12 J. Y. Cherng, T. Y. Hou, M. F. Shih, H. Talsma and W. E. Hennink, *Int. J. Pharm.*, 2013, **450**, 145–162.

13 M. Ding, J. Li, H. Tan and Q. Fu, *Soft Matter*, 2012, **8**, 5414–5428.
14 Y. Xu, X. Wu, X. Xie, Y. Zhong, R. Guidoin, Z. Zhang and Q. Fu, *Polymer*, 2013, **54**, 5363–5373.
15 M. Ding, J. Li, X. He, N. Song, H. Tan, Y. Zhang, L. Zhou, Q. Gu, H. Deng and Q. Fu, *Adv. Mater.*, 2012, **24**, 3639–3645.
16 Z. Pan, L. Yu, N. Song, L. Zhou, J. Li, M. Ding, H. Tan and Q. Fu, *Polym. Chem.*, 2014, **5**, 2901–2910.
17 C. Deng, Y. Jiang, R. Cheng, F. Meng and Z. Zhong, *Nano Today*, 2012, **7**, 467–480.
18 S. Mura, J. Nicolas and P. Couvreur, *Nat. Mater.*, 2013, **12**, 991–1003.
19 R. Cheng, F. Meng, C. Deng, H.-A. Klok and Z. Zhong, *Biomaterials*, 2013, **34**, 3647–3657.
20 E. Fleige, M. A. Quadir and R. Haag, *Adv. Drug Delivery Rev.*, 2012, **64**, 866–884.
21 R. Cheng, F. Feng, F. Meng, C. Deng, J. Feijen and Z. Zhong, *J. Controlled Release*, 2011, **152**, 2–12.
22 L.-Y. Tang, Y.-C. Wang, Y. Li, J.-Z. Du and J. Wang, *Bioconjugate Chem.*, 2009, **20**, 1095–1099.
23 Y.-C. Wang, F. Wang, T.-M. Sun and J. Wang, *Bioconjugate Chem.*, 2011, **22**, 1939–1945.
24 B. Khorsand Sourkohi, A. Cunningham, Q. Zhang and J. K. Oh, *Biomacromolecules*, 2011, **12**, 3819–3825.
25 Y. Zhong, W. Yang, H. Sun, R. Cheng, F. Meng, C. Deng and Z. Zhong, *Biomacromolecules*, 2013, **14**, 3723–3730.
26 J. Wang, G. Yang, X. Guo, Z. Tang, Z. Zhong and S. Zhou, *Biomaterials*, 2014, **35**, 3080–3090.
27 J. Li, M. Huo, J. Wang, J. Zhou, J. M. Mohammad, Y. Zhang, Q. Zhu, A. Y. Waddad and Q. Zhang, *Biomaterials*, 2012, **33**, 2310–2320.
28 Y. Sun, X. Yan, T. Yuan, J. Liang, Y. Fan, Z. Gu and X. Zhang, *Biomaterials*, 2010, **31**, 7124–7131.
29 J. Liu, W. Huang, Y. Pang, P. Huang, X. Zhu, Y. Zhou and D. Yan, *Angew. Chem., Int. Ed.*, 2011, **123**, 9328–9332.
30 P. Sun, D. Zhou and Z. Gan, *J. Controlled Release*, 2011, **155**, 96–103.
31 H. Sun, R. Cheng, C. Deng, F. Meng, A. A. Dias, M. Hendriks, J. Feijen and Z. Zhong, *Biomacromolecules*, 2015, **16**, 597–605.
32 C. Ferris, M. V. de Paz, Á. Aguilar-de-Leyva, I. Caraballo and J. A. Galbis, *Polym. Chem.*, 2014, **5**, 2370–2381.
33 S.-Y. Lee, S. Kim, J. Y. Tyler, K. Park and J.-X. Cheng, *Biomaterials*, 2013, **34**, 552–561.
34 H. S. Han, T. Thambi, K. Y. Choi, S. Son, H. Ko, M. C. Lee, D.-G. Jo, Y. S. Chae, Y. M. Kang and J. Y. Lee, *Biomacromolecules*, 2015, **16**, 447–456.
35 J. Kato, Y. Li, K. Xiao, J. S. Lee, J. Luo, J. M. Tuscano, R. T. O'Donnell and K. S. Lam, *Mol. Pharm.*, 2012, **9**, 1727–1735.
36 Y. Zhong, J. Zhang, R. Cheng, C. Deng, F. Meng, F. Xie and Z. Zhong, *J. Controlled Release*, 2015, **205**, 144–154.
37 X. He, M. Ding, J. Li, H. Tan, Q. Fu and L. Li, *RSC Adv.*, 2014, **4**, 24736–24746.
38 S. Yu, C. He, J. Ding, Y. Cheng, W. Song, X. Zhuang and X. Chen, *Soft Matter*, 2013, **9**, 2637–2645.
39 S. Yu, J. Ding, C. He, Y. Cao, W. Xu and X. Chen, *Adv. Healthcare Mater.*, 2014, **3**, 752–760.
40 S. Zalipsky, C. Gilon and A. Zilkha, *Eur. Polym. J.*, 1983, **19**, 1177–1183.
41 S. Jo and K. Park, *Biomaterials*, 2000, **21**, 605–616.
42 L. Zhou, D. Liang, X. He, J. Li, H. Tan, J. Li, Q. Fu and Q. Gu, *Biomaterials*, 2012, **33**, 2734–2745.
43 L. Zhou, L. Yu, M. Ding, J. Li, H. Tan, Z. Wang and Q. Fu, *Macromolecules*, 2011, **44**, 857–864.
44 T.-G. Iversen, T. Skotland and K. Sandvig, *Nano Today*, 2011, **6**, 176–185.
45 P. Huang, D. Wang, Y. Su, W. Huang, Y. Zhou, D. Cui, X. Zhu and D. Yan, *J. Am. Chem. Soc.*, 2014, **136**, 11748–11756.

